UNIVERSIDAD POLITECNICA DE VALENCIA

ESCUELA POLITECNICA SUPERIOR DE GANDIA

Master en Ingeniería Acústica

UNIVERSIDAD POLITECNICA DE VALENCIA

ESCUELA POLITECNICA SUPERIOR DE GANDIA

Estudio teórico de la dinámica de microburbujas bajo la acción de un campo ultrasónico

TESIS DE MASTER

Autor: Ahmed M.Mehrem

Director: Prof. Víctor J.Sánchez

GANDIA, Julio 2013

THEORETICAL STUDY OF MICROBUBBLE DYNAMICS UNDER THE ACTION OF ULTRASOUND FIELDS

Author:
Ahmed M.Mehrem

Tutor:
Prof. Víctor J. Sánchez Morcillo

Abstract

There are many developments in Ultrasound contrast agents (UCAs) which leads to improvement in medical image. Ultrasound contrast agents are micro scale gas bubbles encapsulated with thin shells on the order of nanometers thick. Therefore, there are many models which describe the behavior of microbubbles in the action of ultrasound. So the study of these models will help us in the future to describe the whole motion of the Microbubble which leads us to a new generation for medical imaging.

Keywords: *Rayleigh-Plesset Equation, UCA Microbubble, Shell Models, Viscos-Elastic Model, Chaotic Motion*

Ahmed Mehrem: Ahmeh@epsg.upv.es

To my parents and my sisters, infinitely grateful
and proud of them.

Acknowledgements

A very special thanks and acknowledge go out to my supervisor, Prof. **Víctor J. Sánchez**, for his patience, motivation, enthusiasm, and immense knowledge, also I want to thank him for his valuable and continuous discussion during the progress of the work and his inspiring me to actually finish.

I am grateful to my friend **Noé Jiménez** for helping me and I hope the best for him in his work and his life.

I deeply thank to my **colleagues** from Department of Applied Physics-EPS de Gandia-UPV for their serious work and for their Continuous cooperation with each other, and I think that they will be the pride of Spain in the future.

I want to thank **Universidad Politécnica de Valencia** to create the right atmosphere for Education and scientific research.

Finally, I would like to thank my beloved country **Egypt** for EVERYTHING.

Ahmed Mehrem

Ahmed Mehrem

Contents

Chapter 3: The chaotic Motion for Microbubble

List of symbols

c	Speed of sound
d	Thickness
$P(t)$	Acoustic driving pressure
P	Pressure
P_{ac}	Acoustic Pressure
P_v	Vapour Pressure
P_G	Gas Pressure
P_∞	Pressure far from the bubble
P_l	Liquid Pressure
P_0	Initial Pressure
R	Bubble radius
R_{01}	Inner Bubble radius
R_{02}	Outer Bubble radius
$\dot{R}$	1st Time derivative for Radius
$\ddot{R}$	2nd time derivative for Radius
V_s	Shell volume
u	Wall bubble velocity
$F(t)$	Function in time
S_p	shell elasticity
S_f	shell friction
R_{buckling}	Below this radius, the surface buckles and $\sigma = 0$
R_{rupture}	Above this radius, the surface ruptures and $\sigma = \sigma_w$
r	Radial distance
t	Time
δ	Damping
δ_{vis}	Viscosity damping
δ_{th}	Thermal damping
δ_{rad}	Radiation damping
δ_t	Total damping
γ	Interfacial tension
κ	Polytropic gas exponent
κ_s	Shell viscosity

ρ	Density
σ	Surface tension
μ	Dynamic viscosity
G_s	elastic modulus
μ_s	shear viscosity
$\sigma_{\text{break-up}}$	Surface tension where surface ruptures
χ	Shell elasticity
ω	Angular frequency

Objective

In this thesis, we will study the behavior of microbubble under the action of ultrasound, this study will include small summary about models of UCAs for encapsulating bubble.

UCAs models are derived for the radius of the bubble as a function of time in response to a time dependent driving pressure. The most fundamental of the nonlinear models is a second order, ordinary differential equation, called the Rayleigh-Plesset (RP) equation.

Models of encapsulating contrast agents are of the utmost importance to understand biomedical signals. The behavior of the encapsulating shell is dependent on the thickness, shear modulus and viscosity of the shell medium. Several models exist for the encapsulating shell.

In this thesis we will study two important models (Hoff and Marmottant), According to parameters of two models we implement a program which describes the behavior of bubble, and we will compare between each model. and then we explain the chaotic motion behavior for microbubble.

Chapter 1

Introduction

1-1 The history of Ultrasound contrast agents

Ultrasound has been widely used in medical practice for at least 50 years. Ultrasound is defined as acoustic waves at frequencies greater than 20 kHz. Natural sources of ultrasound include bats, dolphins and other species that use it for echolocation.

Lord Rayleigh [1] described the gas bubble in acoustic field; Medwin [4] gives an overview of linearized model for scatter and absorption of the sound from the bubble. Prospperetti [1] show nonlinear oscillation of the bubble. But Tucker and wallaby [2] did an experiment to show nonlinear behavior of the bubble and detect of the bubble by receiving scatter at 2nd harmonic of transmit frequency. Imaging at the second harmonic frequency is today commonly used in ultrasound contrast imaging.

Fox and Herzfield [29] showed how an encapsulating shell increases resonance frequency. And then de Jong and Hoff [30] carry out some experiments and then they measured this increased resonance frequency when studying acoustic attenuation from the contrast agent Albunex®.

Hoff and Sontum [5] investigated an experimental contrast agent from Nycomed, using a linear model based on bulk properties of the particles. Holm [2] incorporated these studies into a model for the transmission and scatter of ultrasound pulses in tissue. A more well-founded, nonlinear theoretical model for shell-encapsulated bubbles was presented by Church in 1995. Frinking and de Jong have presented a phenomenological model describing the contrast agent Quantison. All these studies show that the shell increases the mechanical stiffness of the contrast agent particles, and that shell viscosity increases sound absorption.

In the next Table show some product of the Microbubble substance, Manufacturer Company, Gas of the bubble, shell coating and year Manufacturer:

Tab.(1.1)

Name	Manufacturer	Gas	Coating	Approved	Year
Echovist	Bayer Schering Pharma AG	air	galactose	EU, Japan, Canada	1991
Albunex	Molecular Biosystems	air	Human albumin	EU, USA, Canada	1994
Levovist	Bayer Schering Pharma AG	air	galactose, trace palmitin	worldwide1	1996
Optison	GE Healthcare AS	C3F8	Human albumin	EU, USA	1997
Definity	Lantheus Medical Imaging	C3F8	phospholipids	EU, USA, Canada	2001
SonoVue	Bracco	SF6	phospholipids	EU, China, South Am.	2001
Imagent	Alliance Pharmaceutical Corp	C6F14	phospholipids	USA	2002
Sonazoid	Amersham Health	C4F10	lipids	Japan	2006

1: Approved in 65 countries, but not in the USA

1-2 Ultrasound Contrast Agent models

There are different model for the ultrasound contrast agent UCA for the Microbubble, and the different between each shell is the parameters which govern the bubble. For each model, the governing equation of motion for the bubble wall and the constitutive law for the coating material is given.

1-2.1 Free Gas bubble: Rayleigh-Plesset equation

Rayleigh-Plesset (RP) [1,23] equation is a second order nonlinear ODE for the radius of a bubble oscillating in a fluid. The RP equation models for gas bubble in an inviscid and incompressible fluid of constant density ρ.

Liquid

$p_\infty = p_0 + P(t)$ The pressure far from the bubble

$p_L(R, t)$ Liquid pressure at bubble surface

ρ Density of the liquid

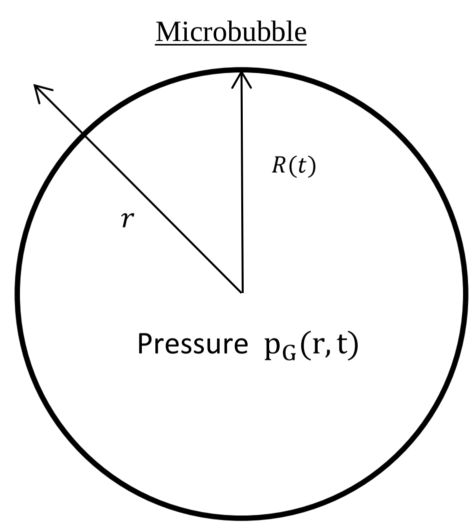

Figure (1.1)

It is assumed that far from the bubble the fluid pressure is p_∞.If there is some driving sound field $P(t)$ the fluid pressure far from the bubble is $p_\infty = p_0 + P(t)$ where p_0 is constant.

$$\ddot{R}R + \frac{3}{2}\dot{R}^2 = \frac{p_l(t) - p_\infty}{\rho} \qquad (1.1)$$

where p_l is the liquid pressure on the surface of the bubble.

Consider a spherically symmetric persistent bubble of radius $R(t)$ as sketched in Figure (1.1) with the bubble center located at the origin, in an infinite domain of inviscid, incompressible, constant density fluid.

By conversion of mass, the inverse-square law requires that the radial outward velocity $u(r,t)$ must be inversely proportional to the square of the distance from the center of the bubble.

There for let $F(t)$ a function of time,

$$u(r,t) = \frac{1}{r^2}F(t) \qquad (1.2)$$

In the case of no mass transport across the boundary, the wall velocity at the boundary is simply the time rate of change of the radius. Thus at the cavity boundary:

$$u(R,t) = \frac{dR}{dt} = \frac{F(t)}{R^2} \qquad (1.3)$$

which give,

$$F(t) = R^2\frac{dR}{dt} \qquad (1.5)$$

In the case where no mass transport occurs, the rate of mass increase inside the bubble is given by

$$\frac{dm}{dt} = \rho_v\frac{dV}{dt} = \rho_v\frac{d(4\pi R^3/3)}{dt} = 4\pi\rho_v R^2\frac{dR}{dt} \qquad (1.4)$$

Where V the volume of the bubble,

$$\frac{dm_l}{dt} = \rho_l A u_l = \rho_l(4\pi R^2)u_l \qquad (1.5)$$

u_l is the velocity of the liquid relative to the bubble at $r = R$,and A is the bubble surface

$$u_l = \left(\frac{\rho_v}{\rho_l}\right)\frac{dR}{dt} \qquad (1.6)$$

Hence

$$u(R,t) = \frac{dR}{dt} - u_l = \frac{dR}{dt} - \left(\frac{\rho_v}{\rho_l}\right)\frac{dR}{dt} = \left(1 - \frac{\rho_v}{\rho_l}\right)\frac{dR}{dt} \qquad (1.7)$$

Therefore

$$F(t) = \left(1 - \frac{\rho_v}{\rho_l}\right)R^2\frac{dR}{dt} \qquad (1.8)$$

The liquid density is much greater than the vapor density $\rho_v \ll \rho_l$, so that F(t)can be approximated by the original zero mass transfer from $F(t) = R^2 \frac{dR}{dt}$ so that

$$u(r, t) = \left(\frac{R}{r}\right)^2 \dot{R} \tag{1.9}$$

where $\dot{R} = \frac{dR}{dt}$. Then, from the spherical symmetric momentum equation and the ideal fluid considered:

$$-\frac{1}{\rho}\frac{\partial p(r,t)}{\partial r} = \frac{\partial u}{\partial t} + u\frac{\partial u}{\partial r} \tag{1.10}$$

Substituting (1.9) into (1.10):

$$-\frac{1}{\rho}\frac{\partial p(r,t)}{\partial r} = \left(\frac{2R\dot{R}^2 + R^2\ddot{R}}{r^2} - \frac{2R^4\dot{R}^2}{r^5}\right) \tag{1.11}$$

Equation (1.11) is then integrated with respect to r from R to ∞, to give equation (3.10).

For convenience assume that the driving field is only applied at $t = 0$ with $P(0) = 0$ and assume that the bubble is initially stationary. The gas within the bubble is modeled as a Polytropic gas. The pressure at the bubble wall will be

$$p(R, t) = p_L(R) = p_G\left(\frac{R_0}{R}\right)^{3\gamma} \tag{1.12}$$

where R_0 is the initial bubble radius and $p_G(0)$ the initial gas pressure. Since the bubble is initially in equilibrium $p_G(0) = p_0$.

Finally upon integrating and applying the boundary conditions:

$$\rho\left(\ddot{R}R + \frac{3}{2}\dot{R}^2\right) = p_0\left(\frac{R_0}{R}\right)^{3\gamma} - p_0 - P(t) \tag{1.13}$$

Which is the simple form for Rayleigh-Plesset Equation.

1-2.2 Models for encapsulating bubble

1-2.2.1 De Jong (1994)

De Jong [2] and his group did some experimental studies in ultrasound contrast agent and modeling by their theoretical description of the vibration of an encapsulated microbubble. This model was about gas bubble in water and the bubble coated by albumin.as any theoretical description for microbubble this model based on Rayleigh-Plesset equation.

From the equation (1.13), the modification of Rayleigh-Plesset Equation will be:

$$\rho_l\left(R\ddot{R}+\frac{3}{2}\dot{R}^2\right)=\left(Po+\frac{2\sigma}{R_0}-p_v\right)\left(\frac{R_0}{R}\right)^{3k}+p_v+\frac{2\sigma}{R}-\frac{4\mu\dot{R}}{R}-p_0-P(t) \qquad (1.14)$$

where p_v is vapor pressure.

In his equation, the viscosity of surrounding liquid is not a separate term as in RP-eq, but it is part of a total damping term δ_t.and liquid viscosity δ_{vis} term thermal δ_{th} and radiation damping δ_{rad} were derived under linear conditions and lumped together in one damping parameter (Medwin, 1977).

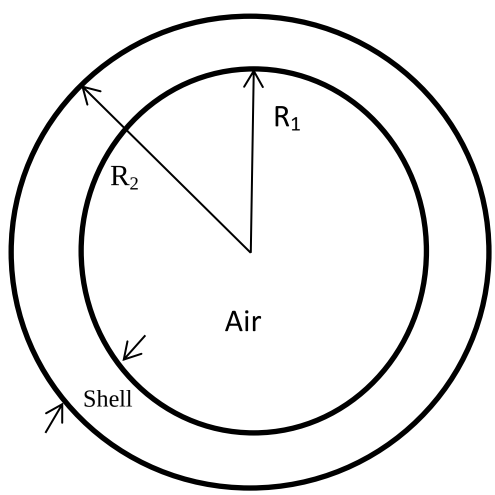

Fig.(1.2) Schematic sketch of an encapsulated bubble.

Their values were determined under linear conditions for Albunex microbubbles by fitting calculated acoustic transmission and scattering values to measurements (de Jong and Hoff, 1993).

$$\rho_l\left(R\ddot{R}+\frac{3}{2}\dot{R}^2\right)=\left(Po+\frac{2\sigma}{R_0}-p_v\right)\left(\frac{R_0}{R}\right)^{3k}+p_v+\frac{2\sigma}{R}-2S_p\left(\frac{1}{R_0}-\frac{1}{R}\right)-\delta_t\omega\rho_l R\dot{R}-|p_0-P(t) \tag{1.15}$$

$$\delta_t=\delta_{rad}+\delta_{vis}+\delta_{th}+\delta_{fr} \tag{1.16}$$

Where S_p is the shell elasticity, δ_t is the total damping, δ_{rad} Radiation damping, δ_{vis} is Viscosity damping, δ_{th} is Thermal damping and δ_{fr} is friction damping

$$\delta_{fr}=\frac{S_f}{4\pi R^3\rho_l\omega} \tag{1.17}$$

where S_f is the shell friction.

1-2.2.2 Church (1995)

Church [2,23] derives his equation from Rayleigh-Plesset model that accounted for the shell thickness and viscoelastic properties.

$$\begin{aligned}\rho_l R\ddot{R}\left(1+(\frac{\rho_l-\rho_s}{\rho_s})\frac{R_1}{R_2}\right)+\rho_s \dot{R}_1^2\left[\frac{3}{2}+\left(\frac{\rho_l-\rho_s}{\rho_s}\right)\left(\frac{4R_2^3-R_1^3}{2R_2^3}\right)\frac{R_1}{R_2}\right] \\ =p_0\left(\frac{R_{01}}{R_1}\right)^{3k}-\frac{2\sigma_1}{R_1}-\frac{2\sigma_2}{R_2}-p_0-p(t)-4\frac{\dot{R}_1}{R_1}\left(\frac{V_s\mu_s+R_1^3\mu_1}{2R_2^3}\right) \\ -4\frac{V_sG_s}{R_2^3}\left(1-\frac{R_{e,1}}{R_1}\right)\end{aligned} \tag{1.18}$$

The subscripts 1 and 2 refer to the inner and outer radius of the microbubble's shell and the subscripts s and L refer to shell and liquid.

$$V_s=R_{02}^3-R_{01}^2 \tag{1.19}$$

G_s is the elastic modulus and μs is the shear viscosity of the shell.

1-2.2.3 Hoff (2000)

Hoff et al. [2,5] derives his model from Church[23] (1995) in the limit of small shell thickness in comparison with the radius. Nycomed is composed of polymer coated, air-filled microbubbles. The shear modulus G_s and viscosity μ_s of a polymeric material are in general frequency dependent, but it is assumed that they are constant for the frequencies considered (1-8 MHz). The following equation of motion was derived,

$$\rho_l\left(R\ddot{R}+\frac{3}{2}\dot{R}^2\right)=Po\left(\left(\frac{R_0}{R}\right)^{3k}-1\right)-P(t)-4\mu_l\frac{\dot{R}}{R}-12\mu_s\frac{d_{s,0}R_0^2}{R^3}\frac{\dot{R}}{R}-12G_s\frac{d_{s,0}R_0^2}{R^3}\left(1-\frac{R_0}{R}\right) \tag{1.20}$$

Where $d_{s,0}$ is the thickness of the shell at the resting state.

1-2.2.4 Morgan (2000)

Morgan [2] constructs his model from Herring equation [4]. Coating effects are represented by two additional terms. The first term is shell term incorporates the elasticity of the shell (χ). The second shell term is a damping term because of the viscosity of the shell (μ_s) and is similar to the derivation of terms by Church (1989). The equation is given by:

$$\begin{aligned}\rho_l\left(R\ddot{R}+\frac{3}{2}\dot{R}^2\right)&\\ &=\left(p_0+\frac{2\sigma}{R_0}+\frac{2\chi}{R_0}\right)\left(\frac{R_0}{R}\right)^{3k}\left(1-\frac{3k}{c}\dot{R}\right)-\frac{4\mu_l\dot{R}}{R}-\frac{2\sigma}{R}\left(1-\frac{1}{c}\dot{R}\right)\\ &-\frac{2\chi}{R}\left(\frac{R_0}{R}\right)^2\left(1-\frac{3}{c}\dot{R}\right)-12\mu_s d_s\frac{\dot{R}}{R(R-d_s)}-p_0-p(t)\end{aligned} \tag{1.21}$$

1-2.2.5 Chatterjee- Sarkar (2003-2005)

Chatterjee-Sarkar [2] used Newtonian interfacial rheological in their model, which means that only viscous interfacial stresses are taken into account. The model considers thin-shelled agents.

$$\rho_l\left(R\ddot{R}+\frac{3}{2}\dot{R}^2\right)=\left(p_0+\frac{2\sigma}{R_0}\right)\left(\frac{R_0}{R}\right)^{3k}-4\mu_l\frac{\dot{R}}{R}-\frac{2\gamma}{R}-\frac{4k_s\dot{R}}{R^2}-p_0-P(t) \qquad (1.22)$$

The material properties were assumed to be independent of the amplitude of oscillation and the transmit frequency (1-10 MHz). The obtained values were $\gamma = 0.9$ N/m and $K_s = 0.08$ kg/s.

1-2.2.6 Marmottant (2005)

Marmottant [2,6] takes into account the physical properties of a lipid monolayer coating on a gas microbubble in his model. Three parameters describe the properties of the shell: a buckling radius, the compressibility of the shell, and a break-up shell tension (χ, k_s, $R_{buckling}$, and $\sigma_{break\text{-}up}$). The model presents an original non-linear behavior at large amplitude oscillations, termed compression-only, induced by the buckling of the lipid monolayer.

$$\rho_l\left(R\ddot{R}+\frac{3}{2}\dot{R}^2\right)=\left(p_0+\frac{2\sigma(R_0)}{R_0}\right)\left(\frac{R_0}{R}\right)^{3k}\left(1-\frac{3k}{c}\dot{R}\right)-p_0-\frac{2\sigma(R_0)}{R}-4\mu_l\frac{\dot{R}}{R}-\frac{4k_s\dot{R}}{R^2}-p(t) \qquad (1.23)$$

This equation is identical to a free gas bubble equation, except from the effective surface tension $\sigma(R)$ term and the shell viscosity term. The surface tension is expressed in terms of the bubble radius:

$$\sigma(R)=\begin{cases} 0 & \text{if } R \le R_{buckling} \\ \chi\left(\dfrac{R^2}{R_{buckling}^2}-1\right) & \text{if } R_{buckling} \le R \le R_{break-up} \\ \sigma_{water} & \text{if ruptured and } R \ge R_{buckling} \end{cases} \qquad (1.24)$$

1-2.2.7 Tsiglifis-Pelekasis (2008)

This model [2] aims to large acoustic pressures for microbubble so Tsiglifis and Pelekasis implement both types of materials in a Keller and Miksis [18] (1980) equation and compare the results with a Kelvin-Voigt [2] based model.

The following nonlinear differential equation describing spherically symmetric oscillations in a compressible liquid is used

$$\left(1 - M\dot{R}'\right)R'\ddot{R}' + \left(\frac{3}{2} - \frac{M\dot{R}'}{2}\right)\dot{R}'^2 = \left(1 + M\dot{R}'\right)\left(p_{l,r=R} - p_0' - P(t)'\right) + MR'\frac{d}{dt}\left(p_{l,r=R} - P(t)'\right) \quad (1.25)$$

1-2.3 Conclusion and Comparison

Now, we have seen different types of ultrasound contrast agent models for encapsulating bubble so we can predict the dynamic behavior for the motion of the bubble under the action of ultrasound. And also we have seen that there are some Models which nearly have different parameters such as the different between Hoff model and Marmottant Model, one of them depend on viscosity and elasticity of the shell substance and the other depend on the buckling and rupture of the shell.

The different between each bubble will help us in the future to create a new model which contains all the parameter and we can predict by behavior of the motion of the bubble.

This table shows the comparison between the models and also governing equations for each model. There are some parameters which govern each model such as elasticity, viscosity, rupture of the shell and buckling radius. Also, the types of the liquid surround the bubble and there are some parameter such as density and viscosity

Author	Year	Governing equation	Constitutive equation
De Jong	1994	Rayleigh-Plesset	Viscoelastic
Church	1995	Rayleigh-Plesset	Kelvin-Voigt
Hoff	2000	Rayleigh-Plesset	Kelvin-Voigt
Morgan	2000	Modified Herring	Viscoelastic
Khismatullin	2002	Keller-Miksis	Kelvin-Voigt
Chatterjee	2003	Rayleigh-Plesset	Newtonian
Allen	2004	Rayleigh-Plesset	neo-Hookean
Sarkar	2005	Keller-Miksis	Viscoelastic
Marmottant	2005	Rayleigh-Plesset	viscolelastic
Doinikov	2007	Rayleigh-Plesset	Maxwell
Stride	2008	Rayleigh-Plesset	viscoelastic
Tsiglifis	2008	Keller-Miksis	Skalak
Tsiglifis	2008	Keller-Miksis	Mooney-Rivlin

Tab.(1.2)

Chapter 2

Simulation programs for the motion of UCAs.

2-1 Simulation program for Radial motion of Microbubble

2-1.1 Rayleigh-Plesset Equation for free gas bubbles

From Rayleigh-Plesset [3] Equation (1.13), we repeat for convenience in (2.1), we will implement a function by using Matlab (Mathworks,) this function depend on two variable which are the radius of the bubble (R) and time (t)

$$\rho\left(\ddot{R}R+\frac{3}{2}\dot{R}^2\right)=p_0\left(\frac{R_0}{R}\right)^{3\gamma}-p_0-P(t) \tag{2.1}$$

We can solve this Equation by using ODEs and we will use ode45 in Matlab, The equation parameters have been set to model an air filled bubble surround by water at ambient temperature and pressure. An overview of the simulation settings is given in Tab. 2.1.

Characteristic values of gas (air) and surrounding liquid (water) that have been used for the simulation (Tab.2.1)

Liquid pressure	p_0	100 kPa
Liquid density	ρ	998 kg/m3
Dynamic liquid viscosity	η	1 mPa
Vapour pressure	p_V	5945 Pa
Surface tension	σ	72.5mN/m
Polytropic exponent	κ	1

The next simulation between two liquid; water with density 1000 kg/m^3 and blood with density 1025 kg/m^3 and we can notice that two line is nearly the same but in the damping the oscillation frequency will change, because of the difference between Blood and water in physical parameters not much different as shown in Tab.(3.2).

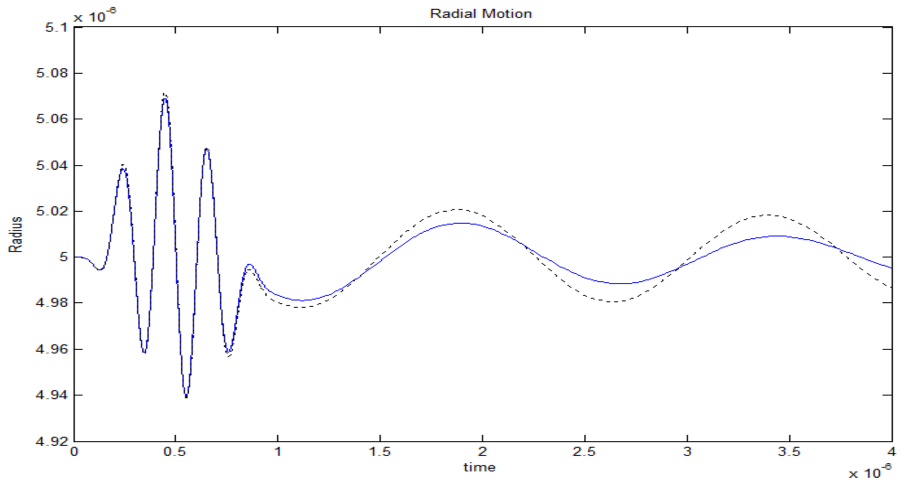

Fig.(2.1) The simulated radial response of a 5μm radius RP air microbubble in Blood (line) water (dots); Hanning pulse with center frequency 5 MHz, 5 cycles in length, 0.3 MPa amplitude.

	Water	**Blood**
Ambient pressure [Pa]	$1.013 * 10^5$	$1.013 * 10^5$
Density of liquid [kg/m3]	1000	1025
Viscosity in liquid [Pas]	$1.0 * 10^{-3}$	$4.0 * 10^{-3}$
Speed of sound in liquid [m/s]	1500	1570

Tab.2.2 Physical parameter for Blood and water

By using the water as liquid, we will increase the pulse amplitude from 300 KPa to 600 KPa we will notice the change in Radius amplitude but in frequency more or less the same.

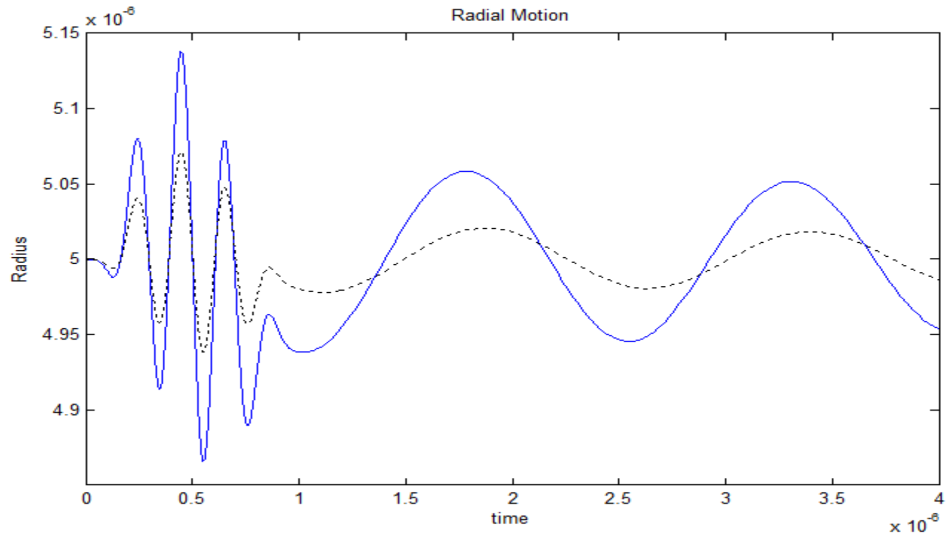

Fig(2.2) The simulated radial response of a 5μm radius RP air microbubble in water ; 300 KPa (dots) 600 KPa (dots); Hanning pulse with center frequency 5 MHz, 5 cycles in length.

Linearization

In the clinical range 2-15 MHz, the primary oscillatory response is linear with the driving Frequency ω Therefore it is useful to linearize the nonlinear ODEs for $R(t)$.

This will give linear ODEs of the generic form [5]

$$\ddot{x} + \beta\dot{x} + \omega_0^2 x = Af(\omega t) \qquad (2.2)$$

where ω_0 is the resonance frequency of the undamped oscillator, β is the constant coefficient of damping. f(t) is a periodic function with frequency ω . A is the amplitude of the forcing term.

And we have pressure P(t) with low amplitude and the radius can be assume to have the form

$$R = R_0(1 + x(t)) \qquad (2.3)$$

where $|x| \ll 1$ and retain only first order terms in x.

From (2.1) Rayleigh-Plesset equation:

$$\ddot{R}R + \frac{3}{2}\dot{R}^2 = \frac{p_0\left(\frac{R_0}{R}\right)^{3\gamma} - p_0 - P(t)}{\rho} \qquad (2.4)$$

Substituting $R = R_0(1 + x(t))$ into the Rayleigh-Plesset equation:

$$\frac{p_0\left(\frac{1}{1+x}\right)^{3\gamma} - p_0 - P(t)}{\rho} = R_0^2(1+x)\ddot{x} + \frac{3}{2}\dot{x}^2 \tag{2.5}$$

Neglecting second order terms in x . This yield:

$$\frac{p_0\left(\frac{1}{1+x}\right)^{3\gamma} - p_0 - P(t)}{\rho} = R_0^2\ddot{x} \tag{2.6}$$

The pressure term is simplified using the binomial theorem:

$$p_0\left(\frac{1}{1+x}\right)^{3\gamma} \approx p_0(1 - 3\gamma x) \tag{2.7}$$

Substitute (2.7) into (2.6), and dividing by R_0^2 to get a familiar equation:

$$\ddot{x} + \frac{3\gamma p_0 x}{\rho R_0^2} = \frac{-P(t)}{\rho R_0^2} \tag{2.8}$$

This is a driven linear oscillator equation with resonant frequency:

$$\omega_0 = \frac{1}{R_0}\sqrt{\frac{3\gamma p_0}{\rho}} \tag{2.9}$$

$$f_0 = \frac{\omega_0}{2\pi} = \frac{1}{2\pi R_0}\sqrt{\frac{3\gamma p_0}{\rho}} \tag{2.10}$$

The simulation below shows the radial motion for Microbubble by linear solution for pulse amplitude 300 KPa and 600 KPa.

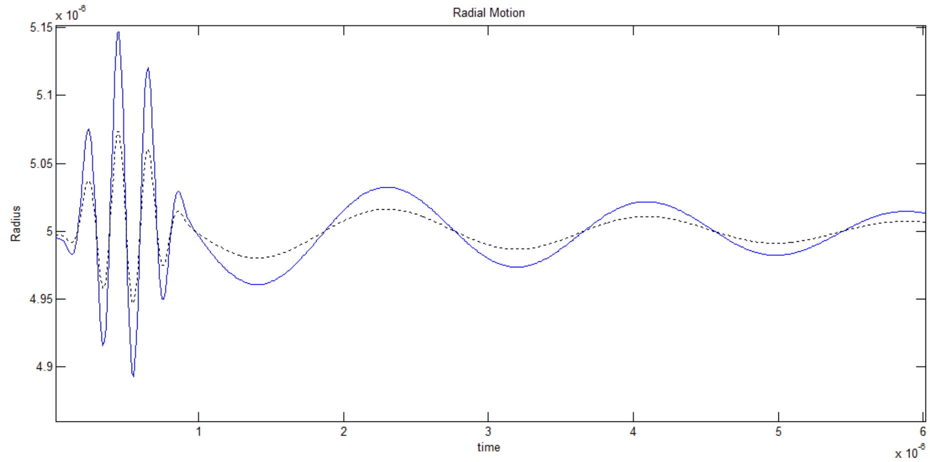

Fig(2.3) The simulation radial response for the solution of linearized equation; where pulse amplitude 300 KPa (dots) and 600 KPa (line) for microbubble radius a 5µm in water to a Hanning pulse with center frequency 5 MHz, 5 cycles in length.

If we compare between the linear solution and Rayleigh-Plesset Equation we will find agreement between the results.

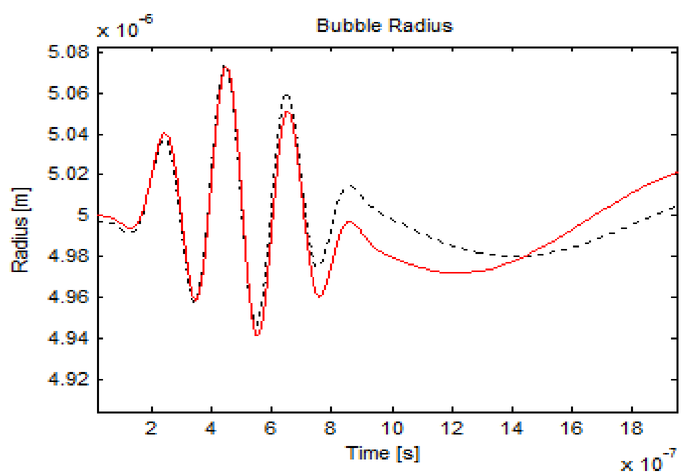

Fig(2.4) The simulation radial response for the solution of linearized (Dots) equation and Rayleigh-Plesset Equation (Line) for microbubble radius a 5µm in water to a Hanning pulse with center frequency 5 MHz, 5 cycles in length; Pulse amplitude 300 KPa

The dimension of Fig(2.3) and Fig(2.4) not the same because of we have to enlarge the graph to obtain a good view.

Resonance frequency

Knowledge of resonant frequencies [5] of contrast microbubbles is important for the optimization of ultrasound contrast imaging and therapeutic techniques. To date, however, there are estimates of resonance frequencies of contrast microbubbles only for the regime of linear oscillation.

For the Equation (2.10) we will calculate the resonance frequency for the bubble with Radius 5μm in fluid density about 1000 kg/m^3, and the pressure 101.3 KPa:

For free bubble (Rayleigh-Plesset Equation):

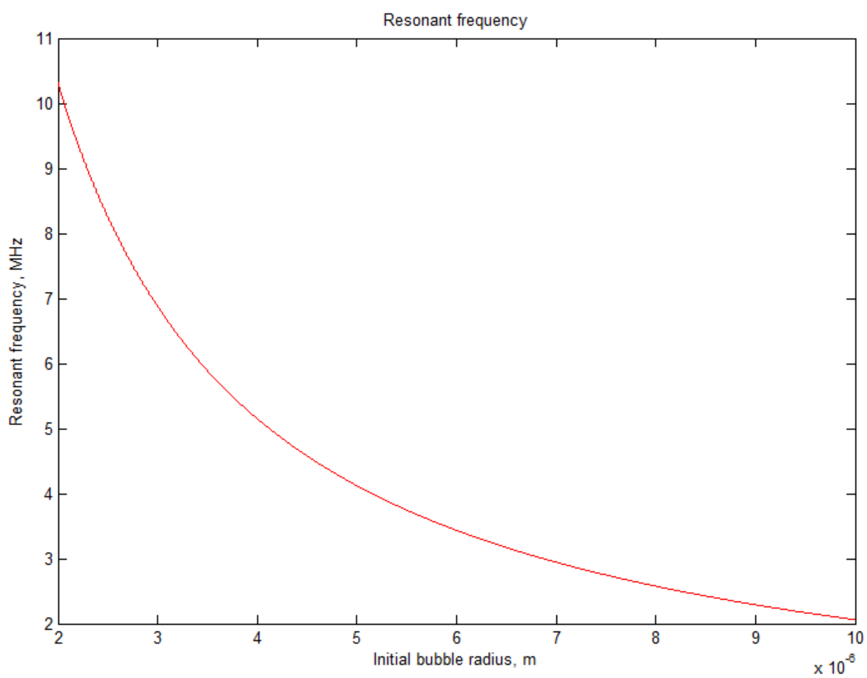

Fig (2.5) Resonance frequency for Rayleigh-Plesset equation; Radius R0=5μm with initial value 2μm, Maximum value 10μm; Fluid density $\rho = 1000\ kg/m^3$

In the Equation (2.10) we will find that the resonance frequency is inversely proportional to the radius of the bubble

$$f_0 \alpha \frac{1}{R_0}$$

As shown in the figure (2.5), increasing in bubble radius decrease the resonance frequency.

We finally compare between the resonance frequency for Rayleigh-Plesset Equation and Church model for encapsulating bubble, and we will find a big difference between them due to the shell term in Church model so the resonance frequency for encapsulating bubble is higher than the free bubble.

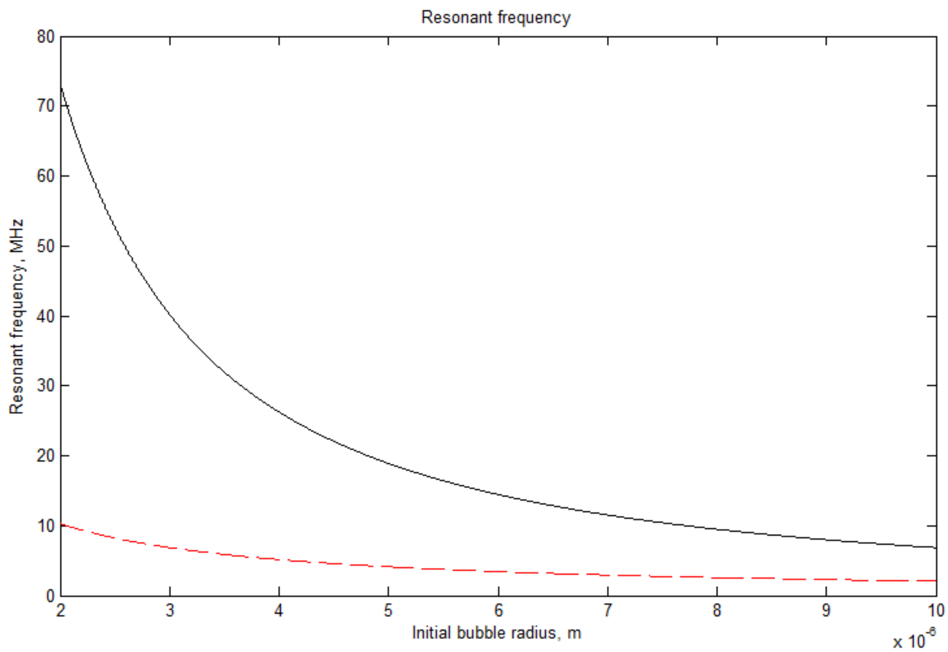

Fig(2.6) The difference between Resonance frequency for Rayleigh-Plesset equation (dash) and church model (line); Radius R_0=5µm with initial value 2µm, Maximum value 10µm; Fluid density $\rho = 1000\ \mathrm{kg/m^3}$

2-2 Numerical analysis for encapsulating bubble with Viscous-Elastic properties (Hoff's Model)

2-2.1 Equation of Motion for Microbubble

Assume that we have a bubble with radius R and the shell thickness ds which not exceed 5% of the whole bubble. This bubble in a liquid with viscosity μ_L, and density $\rho_L$in the action of ultrasound as shown in figure (2.7). Frequency Range in Medical imaging applications (2 MHz to 15 MHz).

Figure 2.7

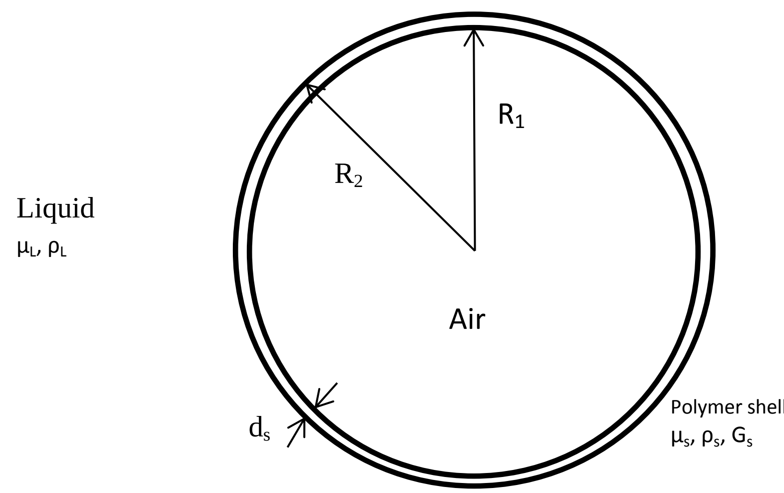

- → Bubble Diameter (1μm to 10μm)
- → The Shell thickness 5% of the Particle radius.
- → The shell reduce surface tension at the Shell-liquid and Shell-gas interfaces so we can neglect the

Figure (2.7)

where d_{se} is the shell thickness at rest,

The nonlinear equation of motion [5] for Church Model for the bubble surface is

$$\rho_l\left(\ddot{R}_2R_2+\frac{3}{2}\dot{R}_2^2\right)+\rho_s\left(\ddot{R}_2R_2\left(\frac{R_2}{R_1}-1\right)+\dot{R}_2^2\left(2\frac{R_2}{R_1}-\frac{1}{2}\left(\frac{R_2}{R_1}\right)^4-\frac{3}{2}\right)\right)$$
$$=p_{ge}\left(\frac{R_{1e}}{R_1}\right)^{3k}-p_\infty(t)-4\mu_l\frac{\dot{R}_1}{R_1}-4G_s\frac{V_s}{R_2^3}\left(1-\frac{R_{1e}}{R_1}\right) \quad (2.11)$$

where $R_1(t)$ and R_2 (t) are the inner and outer shell radii, $\rho_s$and ρ_l are the densities of the shell material and of the surrounding liquid, $p_{ge}$is the equilibrium pressure in the gas inside the bubble, R_{1e} and R_{2e} are the inner and outer shell radii at equilibrium, p_∞ (t) is the pressure in the liquid far from the particle, k is the polythropic exponent of the gas,

$$V_s=R_2^3-R_1^3 \quad (2.12)$$

Equation (2.11) is Church's Eq. we have to modify this Equation to identify the different terms, using the conservation of mass relation for an incompressible shell;

$$\dot{R}_1 R_1^2 = \dot{R}_2 R_2^2 \tag{2.13}$$

According to this description, the thickness d_s of the shell varies as the particle oscillates, so that the shell volume is constant. The shell is thin compared to particle radius, and use of this, $d_s(t) \ll R$ allows simplification of Equation (2.11).

Now, Equation (2.11) contains different terms. The left side consist of inertia of shell, inertia of liquid and $\rho_s$and ρ_l and we have to simplify this term

$$\rho_l \left(\ddot{R}_2 R_2 + (1 + \frac{\rho_s}{\rho_l} \frac{d_s}{R_2}) \frac{3}{2} \dot{R}_2^2 \right) \tag{2.14}$$

Hence, the shell contributes to the inertia of the oscillating bubble through a term of order d_s/R_2, which can be neglected.

The right side of Equation (2.11) represents restoring stiffness and damping viscous forces. The first three terms are known from the Rayleigh–Plesset equation for unshelled bubbles.

The last two terms represent viscous and elastic forces due to movement and tension in the shell. The shell is thin, and terms of order d_s/R_2 are neglected. This reduces the last two terms in Equation (2.11) to

$$4\mu_l \frac{V_s}{R_2^3} \frac{\dot{R}_1}{R_1} \approx 12\mu_l \frac{R_{1e}^2 d_{se}}{R_2^3} \frac{\dot{R}_1}{R_1} \tag{2.15}$$

$$4G_s \frac{V_s}{R_2^3} \left(1 - \frac{R_{1e}}{R_1}\right) \approx 12G_s \frac{R_{1e}^2 d_{se}}{R_2^3} \left(1 - \frac{R_{1e}}{R_1}\right) \tag{2.16}$$

While the shell contribution to inertia is small and neglected, the contributions from the shell to stiffness and viscosity depend on shear modulus G_s and shell viscosity μ_s, and must be considered.

The result of these simplifications is a version of Equation (2.11) suitable when the encapsulating shell is thin compared to the particle diameter.

$$\rho_l\left(\ddot{R}_2 R_2 + \frac{3}{2}\dot{R}_2^2\right) = p_{ge}\left(\frac{R_{1e}}{R_1}\right)^{3k} - p_\infty(t) - 4\mu_l\frac{\dot{R}_1}{R_1} - 12G_s\frac{R_{1e}^2 d_{se}}{R_2^3}\left(1 - \frac{R_{1e}}{R_1}\right) - 12\mu_l\frac{R_{1e}^2 d_{se}}{R_2^3}\frac{\dot{R}_1}{R_1} \qquad (2.17)$$

Equation (2.17) contains both inner radius $R_1$and outer radius R_2 of the shell. It is reduced to an equation in outer radius $R = R_2(t)$ alone by setting

$$\frac{R_{1e}}{R_1} \approx \frac{R_{2e}}{R_2}\left(1 + \left(\frac{d_{se}}{R_{2e}} - \frac{d_s}{R_2}\right)\right) \approx \frac{R_{2e}}{R_2} = \frac{R_e}{R} \qquad (2.18)$$

At equilibrium, the pressure in the gas inside the bubble is assumed to be equal to the hydrostatic pressure in the surrounding liquid, $p_{ge} = p_0$.

$$\rho_l\left(R\ddot{R} + \frac{3}{2}\dot{R}^2\right) = Po\left(\left(\frac{R_0}{R}\right)^{3k} - 1\right) - P(t) - 4\mu_l\frac{\ddot{R}}{R} - 12\mu_s\frac{d_{s,0}R_0^2}{R^3}\frac{\dot{R}}{R} - 12G_s\frac{d_{s,0}R_0^2}{R^3}\left(1 - \frac{R_0}{R}\right) \qquad (2.19)$$

This is equation for Hoff model and we have to solve it. To simulate bubble oscillation $R(t)$ as a response to an applied acoustic pressure field $p_i(t)$, the elastic and viscous shell parameters G_s and μ_s must be determined. The shell material is not easily made in bulk quantities that allow conventional measurements of elastic properties. Instead, G_s and μ_s are estimated from measurements of ultrasound absorption in a particle suspension.

Linearization

The parameters G_s and μ_s are estimated from acoustic measurements at low pressure amplitudes. Here, the oscillation is linear and Equation (2.19) is solved analytically. The particle radius R(t) is written

$$R(t) = R_e\left(1 + x(t)\right), \quad |x(t)| \ll 1 \qquad (2.20)$$

Equation (2.19) is expanded in the radial displacement $x(t)$,

$$mR_e\ddot{x} + R'R_e\dot{x} + sR_e x = -4R_a^2 p_i(t) \qquad (2.21)$$

With Coefficients

$$m = 4\pi\rho_l R_e^3 \qquad (2.22)$$

$$s = 4\pi R_e\left(4kp_0 + 12G_s\frac{d_{se}}{R_e}\right) \qquad (2.23)$$

$$R' = 4\pi R_e\left(4\mu_l + 12\mu_s\frac{d_{se}}{R_e}\right) \qquad (2.24)$$

Equation (2.21) is best handled in the frequency domain. Fourier transformation yields

$$(\omega_0^2 - \omega^2 + i\omega\omega_0\delta)\hat{x}(\omega) = -\frac{1}{\rho_l R_e^2}\hat{p}_i(\omega) \qquad (2.25)$$

With Coefficients

$$\omega_0^2 = \frac{s}{m} = \frac{1}{\rho_l R_e^2}\left(3kp_0 + 12G_s\frac{d_{se}}{R_e}\right) \qquad (2.26)$$

$$\delta = \frac{R}{\omega_0 m} = \delta_l + \delta_s \qquad (2.27)$$

$$\delta_l = \frac{4\mu_l}{\omega_0 \rho_l R_e^2} \tag{2.28}$$

$$\delta_s = \frac{4\mu_s \frac{d_{se}}{R_e}}{\omega_0 \rho_l R_e^2} \tag{2.29}$$

The linear resonance frequency $f_0$of the shell encapsulated bubble is

$$f_0 = \frac{\omega_0}{2\pi} = \frac{1}{2\pi R_e}\sqrt{\frac{1}{\rho_l}\left(3kp_0 + 12G_s\frac{d_{se}}{R_e}\right)} \tag{2.30}$$

From the equation (2.10) which describes the resonance frequency of free bubble and compare with (2.30) we will find adding of shell term $12G_s\frac{d_{se}}{R_e}$, the graph below shows the difference between resonance frequency of Rayleigh-Plesset equation (free bubble) and the resonance frequency of encapsulating bubble models.

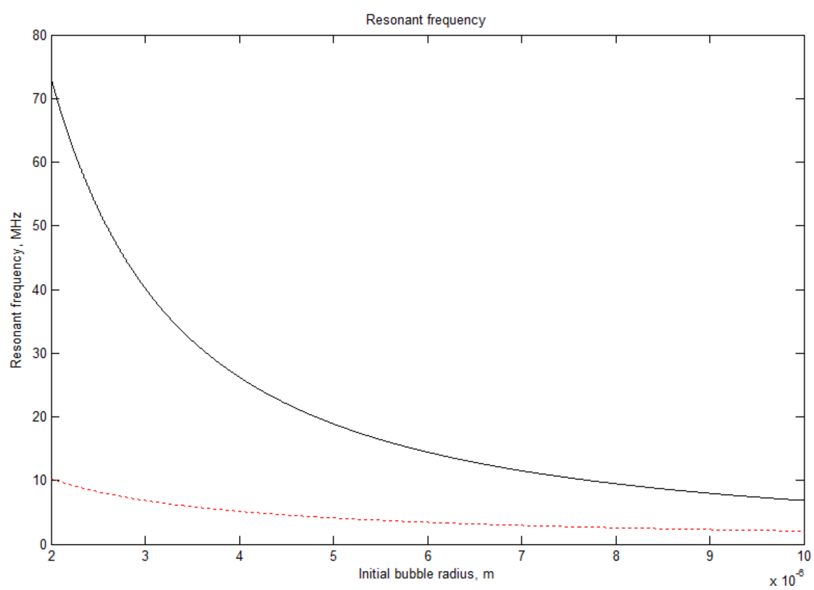

Fig(2.8) Resonant frequency as a function of initial bubble radius R_0=2:10 µm for 3 different bubble models. Rayleigh-Plesset equation (Dots) and shell model (Line)

2-2.2 Simulation Program for Hoff Model

Hoff solved this model numerically by using Matlab (package BubbleSim) and he simulated the behavior of bubble motion in the action of ultrasound. As we know Hoff's model depend on some parameters which is the viscosity and elasticity of the shell.

The Table below shows the value of each parameter and the liquid surrounding the bubble:

Parameters and Values(Tab 2.3)

Parameter	**Value**	**Description**
p_0	1.013 x 105 Pa	Ambient pressure
ρ	1000 kg/m3	Density of liquid
γ	1.4	Polytropic exponent
	Shell parameters Albunex©	
δ	15 nm	Shell thickness
G_s	88,8 MPa	Shell elastic modulus
μ_s	0,5 Pa s	Shell viscosity
σ	7 Pa m	Surface Tension
	Nycomed©	
δ	250 nm	Shell thickness
G_s	11 MPa	Shell elastic modulus
μ_s	0,45 Pa s	Shell viscosity
σ	7 Pa m	Surface Tension
	Sonazoid©	
δ	4 nm	Shell thickness
G_s	50 MPa	Shell elastic modulus
μ_s	0.8 Pa s	Shell viscosity

Hoff used Stiff ordinary diffraction equations to solve the Equation by using (*ode15s*) code. This model based on the Solution of Rayleigh-Plesset Equation and also modified by adding the viscosity and elasticity parameters term.

The table below shows Bulk modulus of for different shell:

Particle stiffness. Bulk modulus of the investigated polymer shelled Particles compared with other substances. Tab.(2.4)

Substance	Bulk modulus K[MPa]
Air (isothermal)	0.10
Air (adiabatic)	0.14
Polymer-shelled air bubbles	2.5
Water	2250
Steel	160 000

The acoustic pressure is function was Sinusoid with angular frequency ω. The Hanning window of width x, was chosen as it is a typical medical ultrasound pulse.

$$\omega(x) = \frac{1}{2}(1 + \cos(x)) \qquad (2.31)$$

Results are stored in the Matlab *struct*-variables; *pulse*: Driving ultrasound pulse; *particle:* Parameters of the contrast agent particle, or bubble; *linear:* Results of linear calculation; *simulation*: Results of nonlinear simulation; *graph* Plotting and saving parameters

For example we will take Sonazoid© and Albunex© for describe the simulation,

Simulation for **Sonazoid**©:

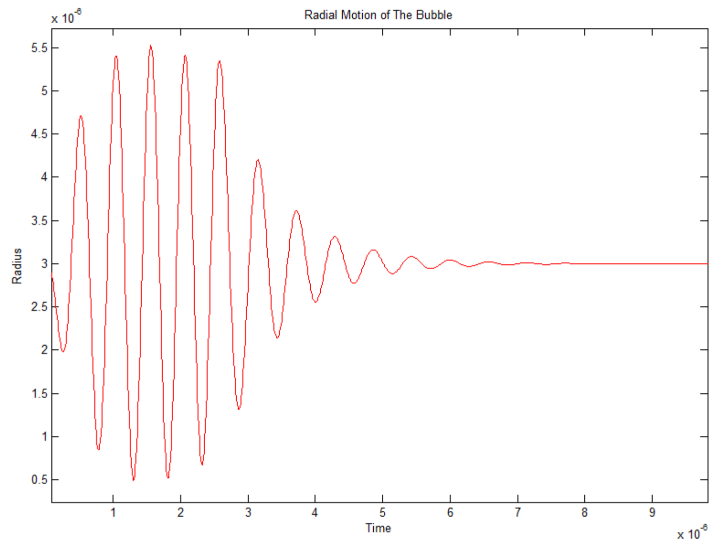

Fig(2.9) Bubble response for Hoff Model for Water; Radius R_0=3μm; pulse amplitude=0.3 MPa; Pulse length 5 cycles under frequency 2 MHz: shell Parameter for shear modulus 50 MPa, shell viscosity 0.8 Pas and shell thickness 4 nm

The power spectrum is the amplitude of the discrete Fourier transform of the driving pulse and the scattered pulse. The spectrum shows the amplitude of the various frequency responses of the bubble radius. Hence, the linear response and the higher and possibly subharmonics may be observed.

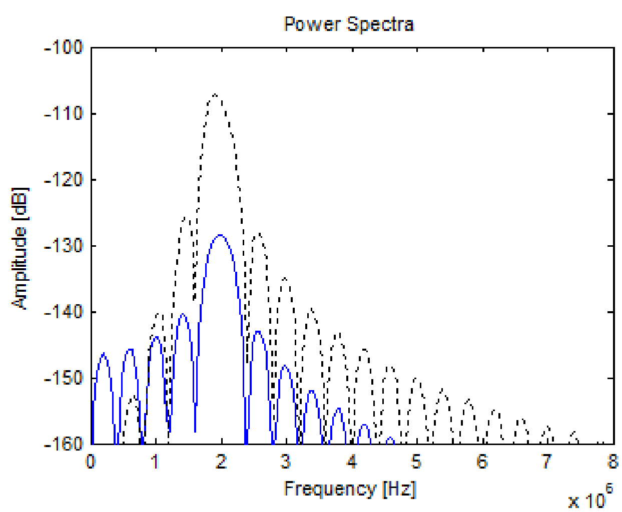

Fig(2.10) Power spectra for Hoff Model for Water; Radius R_0=3μm; pulse amplitude=0.3 MPa; Pulse length 5 cycles under frequency 2 MHz: shell Parameter for shear modulus 50 MPa, shell viscosity 0.8 Pas and shell thickness 4 nm

For Albunex©:

Albunex [24] is a new ultrasound contrast agent for medical imaging. The product consists of air-filled albumin microspheres suspended in a solution of 5% (w/v) human albumin. The suspension is sterile and a viscosity of 1.4 relative to water. The contrast effect is caused by the air-filled microspheres, which range in diameter from 1 to 15 microns, with less than 5% being larger than 10 microns.

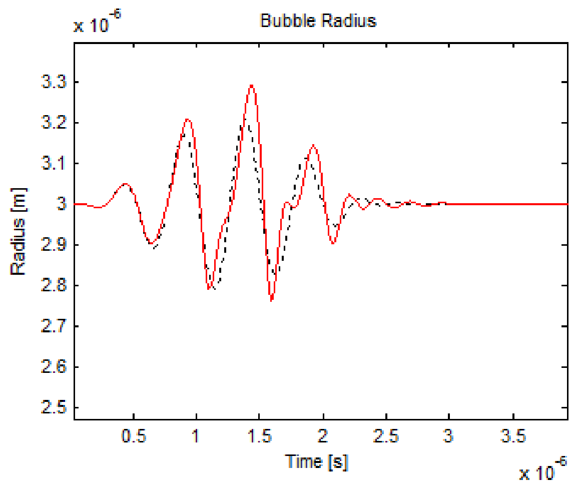

Fig(2.11) Bubble response for Hoff Model; Simulation (Line), Linearization (Dots); Radius R_0=15μm; pulse amplitude=0.3 MPa; Pulse length 5 cycles under frequency 2 MHz: shell Parameter for shear modulus 88.8 MPa, shell viscosity 0.7 Pas and shell thickness 15 nm

The relation between Amplitude and frequency shows that there are a large difference between linearize equation and Hoff model as shown in the figure

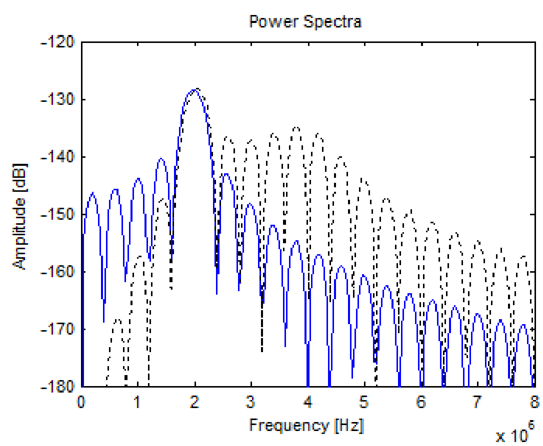

Fig(2.12) Power Spectra for Hoff Model; Simulation (Line), Linearization (Dots); Radius R_0=15μm; pulse amplitude=0.3 MPa; Pulse length 5 cycles under frequency 2 MHz: shell Parameter for shear modulus 88.8 MPa, shell viscosity 0.7 Pas and shell thickness 15nm

2-2.3 Conclusion

Hoff Model has been developed describing oscillations of gas bubbles encapsulated in a thin polymer shell. Hoff model depends on viscoelastic parameters of the shell material.

A linearized version of the model was used to estimate the shell material properties shear modulus and shear viscosity from acoustic attenuation spectra.

This study shows the week point between linear solution and theoretical Model. The results show that the polymer shell increases particle stiffness 20 times compared to a free gas bubble.

The fundamental assumptions of the models, such as spherically symmetric and stationary bubbles are unrealistic for contrast agents in the body. Smaller blood vessels are often of comparable size to the microbubble and the presence of boundaries will break the spherical symmetry.

Blood is also much more viscous with a slightly higher sound speed than water. The red blood cells are of comparable size to the contrast agent, hence there will be collisions between the cells and the contrast agents.

2-3 Numerical analysis for buckling and rupture properties (Marmottant's Model)

2-3.1 Equation of motion of the particle

Marmottant [6] model based on Rayleigh-Plesset equation (1.13) in phospholipid coated microbubble at large amplitude. By count the surface tension which depends on the molecule substance.

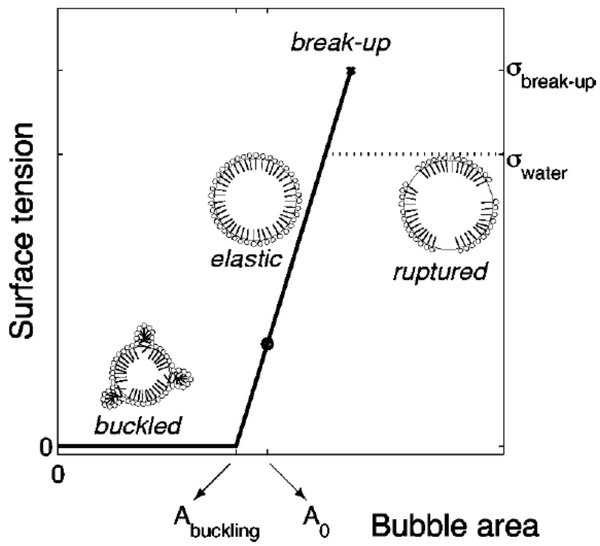

Fig(2.13)

This model has three parameters to describe the surface tension: the buckling area of the bubble $A_{buckling}$ as shown the fig.(2.13) when the surface buckles, an elastic modulus χ that gives the slope of the elastic regime. The third parameter which to describe the moment of rupture: the elastic regime holds until a critical break-up tension called $\sigma_{break-up}$. When this limit has been reached the maximum surface tension saturates at σ_{water}.

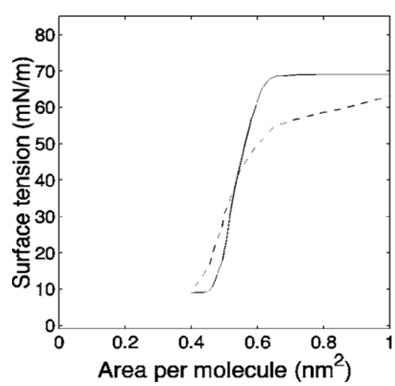

Fig(2.14)the relation between Surface tension and Area per molecule

We motivate here the modeling of the three states:

- $\boxed{\text{Buckled state, } \sigma = 0}$.

We assume a near vanishing surface tension in the buckled state.

The buckling area of the bubble depends on the number n of lipid molecules at the interface and on the molecular area at buckling $a_{buckling}$

$$A_{buckling} = n\, a_{buckling} \qquad (2.32)$$

And we can consider that

$$a_{buckling} = 0.4 \text{ nm}^2$$

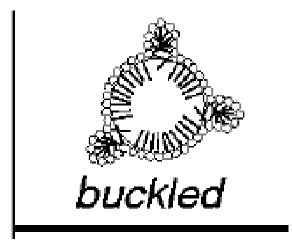

- $\boxed{\text{Elastic state,} \sigma = \chi\left(\frac{A}{A_{buckling}} - 1\right)}$

This is the area between Buckling and rupture. The lower limit for this area is $A_{buckling}$ and the Upper limit is the maximum surface tension which depend on the substance molecule, which is $\sigma_{break\ up}$ before rupture of the shell giving

$$R_{break\ up} = R_{buckling}\left((1 + \sigma_{break\ up} / \chi)\right)^{1/2} \qquad (2.33)$$

Or σ_{water} after rupture giving

$$R_{rupture} = R_{buckling}((1 + \sigma_{water} / \chi))^{1/2} \qquad (2.34)$$

The elastic regime holds only in a narrow range of radii, since χ is usually large compared to $\sigma_{\text{break up}}$ or σ_{water}. The value of the elastic modulus can also incorporate the presence of any solid-like shell material that sustains tensile stress.

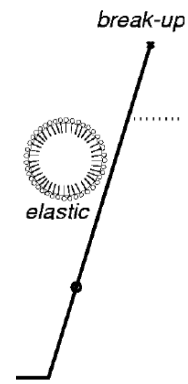

Within this regime the surface tension is a linear function of the area, or of the square of the radius, and for small variations around a given radius R0, it can be written as:

$$\sigma(\mathrm{R}) = \sigma(\mathrm{R}_0) + \chi\left(\frac{\mathrm{R}^2}{\mathrm{R}_0^2} - 1\right) \cong \sigma(\mathrm{R}_0) + 2\chi\left(\frac{\mathrm{R}}{\mathrm{R}_0} - 1\right) \qquad (2.35)$$

When

$$|\mathrm{R} - \mathrm{R}_0| \ll \mathrm{R}_0$$

- $\boxed{\text{Ruptured state, } \sigma = \sigma_{\text{water}}}$

A fast expansion, such as the one triggered on a bubble by an ultrasonic pressure pulse, does not allow much time for any phase change and the monolayer is likely to break at a critical tension $\sigma_{\text{break up}}$, exposing bare gas interfaces to the liquid.

The bare interface has a tension value of σ_{water}. The break-up tension can be higher than σ_{water}, since any polymer component confers more cohesion to the shell, and shifts the break-up to higher tensions.

The introduction of a high tension break-up was motivated by the observation of resistant bubbles, as will be exposed further.

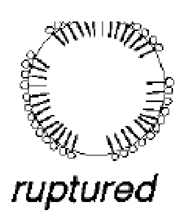

Whereas the elasticity of the coating depends on the bubble radius, the viscosity remains constant. The modified Rayleigh-Plesset equation by Keller and Miksis [2] (1980) was used.

$$\rho_l\left(R\ddot{R}+\frac{3}{2}\dot{R}^2\right)=\left(p_0+\frac{2\sigma(R_0)}{R_0}\right)\left(\frac{R_0}{R}\right)^{3k}\left(1-\frac{3k}{c}\dot{R}\right)-p_0-\frac{2\sigma(R_0)}{R}-4\mu_l\frac{\dot{R}}{R}-\frac{4k_s\dot{R}}{R^2}-p_{ac}(t) \tag{2.36}$$

This is the equation of motion for Marmottant model, where $p_{ac}(t)$ is acoustic pressure .

This equation is identical to a free gas bubble equation, except from the effective surface tension $\sigma(R)$ term and the shell viscosity term. The surface tension is expressed in terms of the bubble radius:

$$\sigma(R)=\begin{cases}0 & \text{if } R \le R_{buckling} \\ \chi\left(\dfrac{R^2}{R_{buckling}^2}-1\right) & \text{if } R_{buckling} \le R \le R_{break-up} \\ \sigma_{water} & \text{if ruptured and } R \ge R_{buckling}\end{cases} \tag{2.37}$$

Shell parameters (elasticity χ, viscosity k_s, buckling radius $R_{buckling}$, and $\sigma_{break\text{-}up}$) were determined by fitting to optical recordings of vibrating contrast agent microbubbles.

Simulation Program for Marmottant Model

The models derived were solved numerically using the Mathematica (Wolfram, Version 8) simulation of ultrasound contrast agents. The parameters for the liquid, gas and shell, if present, are shown in Table below. All the solutions assume an adiabatic process, containing air, and the external liquid is water.

Magnitude	Value
Acoustic pressure P_a (Pa)	130*10^{3}
Initial radius R_0 (m)	0.975*10^{-6}
Shell viscosity κ_s (N)	15*10^{-9}
Central frequency f (Hz)	2.9*10^{6}
Shell elasticity χ (N/m)	1
Interfacial tension γ (N/m)	1.07
liquid density ρ_l (Kg/m^3)	1000
Surface tension of liquid σ_l (N/m)	0.072
Speed of sound c (m/s)	1480

Tab. (2.5) Marmottant Parameters

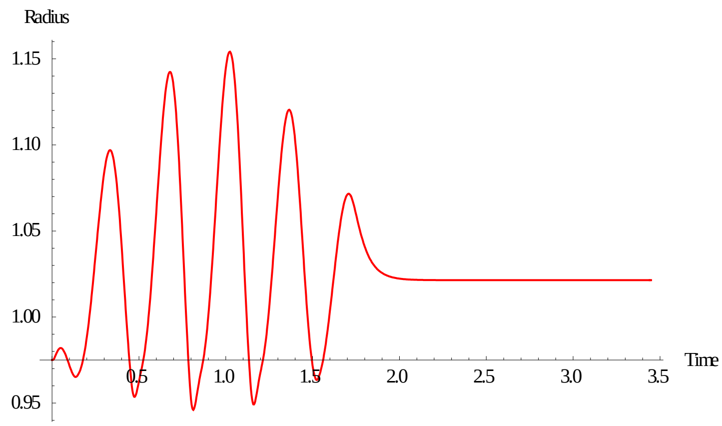

Fig(2.15) Radius-time curve (radius in microns, time in microseconds) for Marmottant Model; Radius Buckling R_0=0.975 µm; $f = 2.9 * 10^6$; χ=1 N/m; ks=15x10-9 N; $\sigma_{break\ up}$>1 N/m; Liquid density $\rho_l = 1000\ Kg/m^3$; c=1480 m/s and polytrophic gas exponent is k=1.095

The next graph describe the relation between Amplitude (40 KPa) and timefor bubble with radius $R_0 = 0.975\ \mu m$. the Liquid density $\rho_l = 1000\ Kg/m^3$.

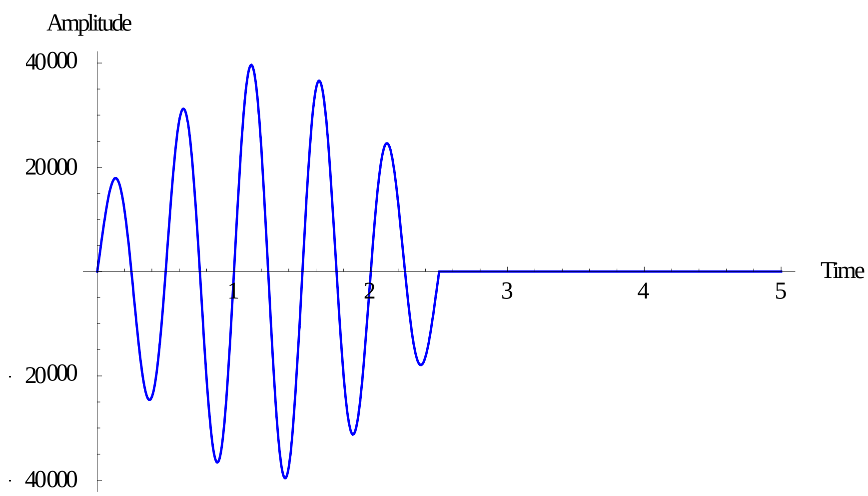

Fig(2.16) Driving pressure (amplitude in Pa, time in microseconds) for Marmottant Model; Radius Buckling R0=0.975 µm; $f = 2.9 * 10^6$; χ=1 N/m; ks=15x10-9 N; $\sigma_{break\ up}$>1 N/m; Liquid density $\rho_l = 1000\ Kg/m^3$; c=1480 m/s and polytrophic gas exponent is k=1.095

scattering of phospholipid-shell [30] microbubbles excited at relatively low acoustic pressure amplitudes (<30 kPa) has been associated with echo responses from compression-only bubbles having initial surface tension values close to zero(30).

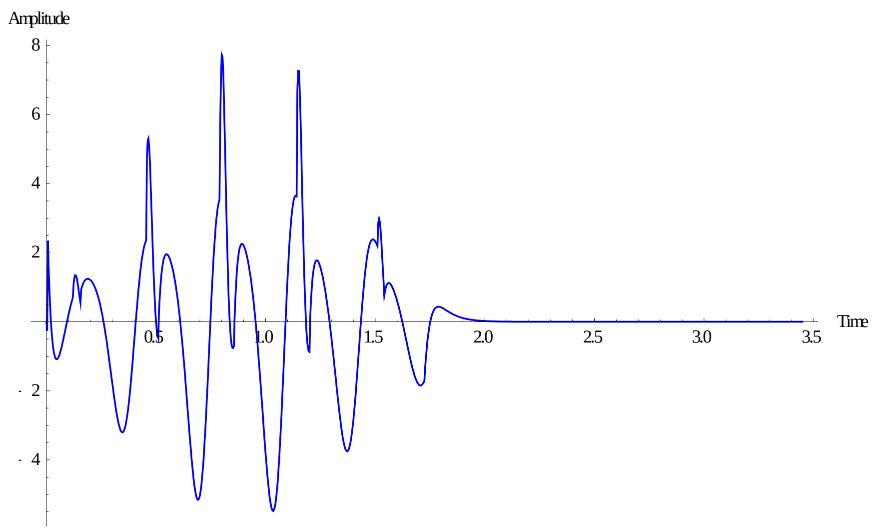

Fig(2.17) Scattered pressure-time curve at L = 0.01 m (amplitude in Pa, time in microseconds) for Marmottant Model; Radius Buckling R_0=0.975 µm; $f = 2.9 * 10^6$; χ=1 N/m; ks=15x10-9 N; $\sigma_{break\ up}$>1 N/m; Liquid density $\rho_l = 1000\ Kg/m^3$; c=1480 m/s and polytrophic gas exponent is k=1.095

Conclusion

The behavior of the coated microbubble in an ultrasound field was studied. We presented a simple model for the dynamical properties of coated contrast agents bubbles, with three parameters: a buckling surface radius, a shell compressibility, and a break-up shell tension. It predicts a compression-only behavior of the bubble, a highly non-linear response. It occurs when its radius is close to the buckling radius, a state that naturally occurs with dissolution of gas, or that can be accelerated by repeated pulses.

High-frequency image recordings with lipid coated microbubbles reveal the existence of such asymmetric oscillations, and validate the model. The break-up of the shell is modeled by a third parameter, a finite tension of the bubble shell above which bare interfaces are created, with a corresponding change in bubble dynamics.

Chapter 3

The Chaotic Motion of Microbubble

2-1 Introduction

The dynamics of UCAs are inherently nonlinear and an understanding of the response to ultrasound is necessary to enable the effective use of UCAs in clinical applications. The purpose of this chapter is to develop an understanding of the nonlinear dynamics of UCAs subject to acoustic forcing for various types of shells under typical clinical conditions in frequency 2 MHz. This understanding will aid in the selection of shell materials, ultrasound frequency, and forcing amplitude for a particular application.

2-2 The Chaotic Motion of Microbubble

The nonlinear response of spherical ultrasound contrast agent microbubbles is investigated to understand the effects of common shells on the dynamics. A compressible form of the Rayleigh–Plesset equation is combined with a thin-shell model developed by Lars Hoff to simulate the radial response of contrast agents subject to ultrasound. Parameters of the shell in table (2.3).

In Figure (3.1) shows the relation between Radius-Time in pulse amplitude 300 KPa which we can notice that the relation is harmonic, periodic and has one peak, and if we increase pulse amplitude to 400 KPa the relation will also be periodic but it has two different peak. By increasing the pulse amplitude again, we will find that the bubble starts in a chaotic motion as shown in the figure (3.1) and (3.2).

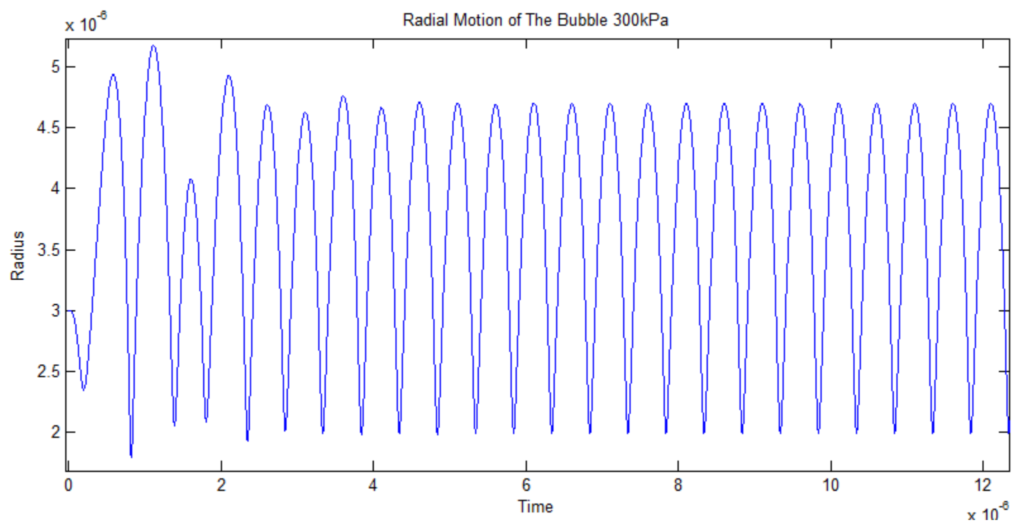

Fig(3.1) The simulated radial response of a 3µm radius for microbubble in water to a rectangular pulse with center frequency 2 MHz; Amplitude 0.3 MPa.

The next relation between the velocity of the shell and the Radius, the small line inside the graph describes irregular motion (as shown in Fig. 3.1) and then a dense line shows the harmonic and periodic behavior.

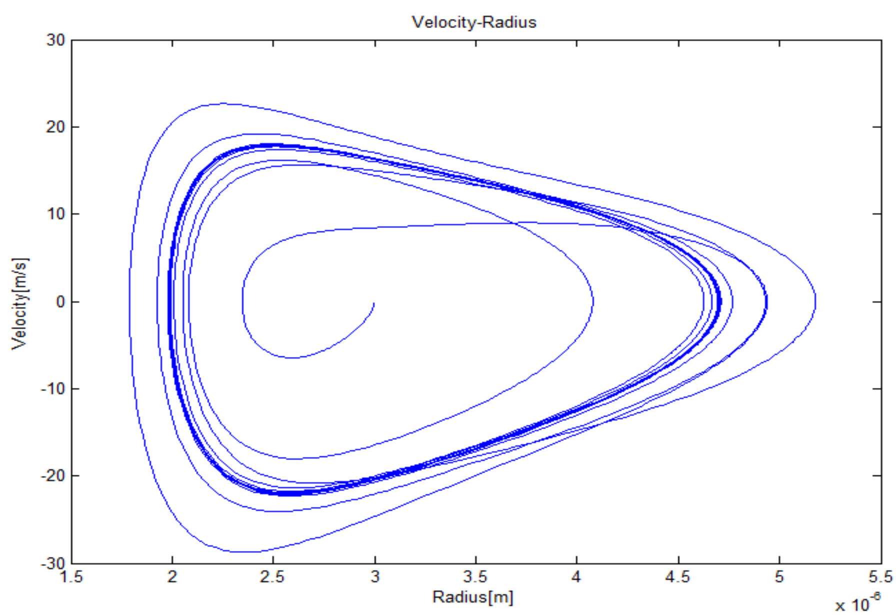

Figure (3.2) Phase portraits of Sonazoid© UCA with f = 2 MHz, ae=3 µm, for Pac =300 kPa

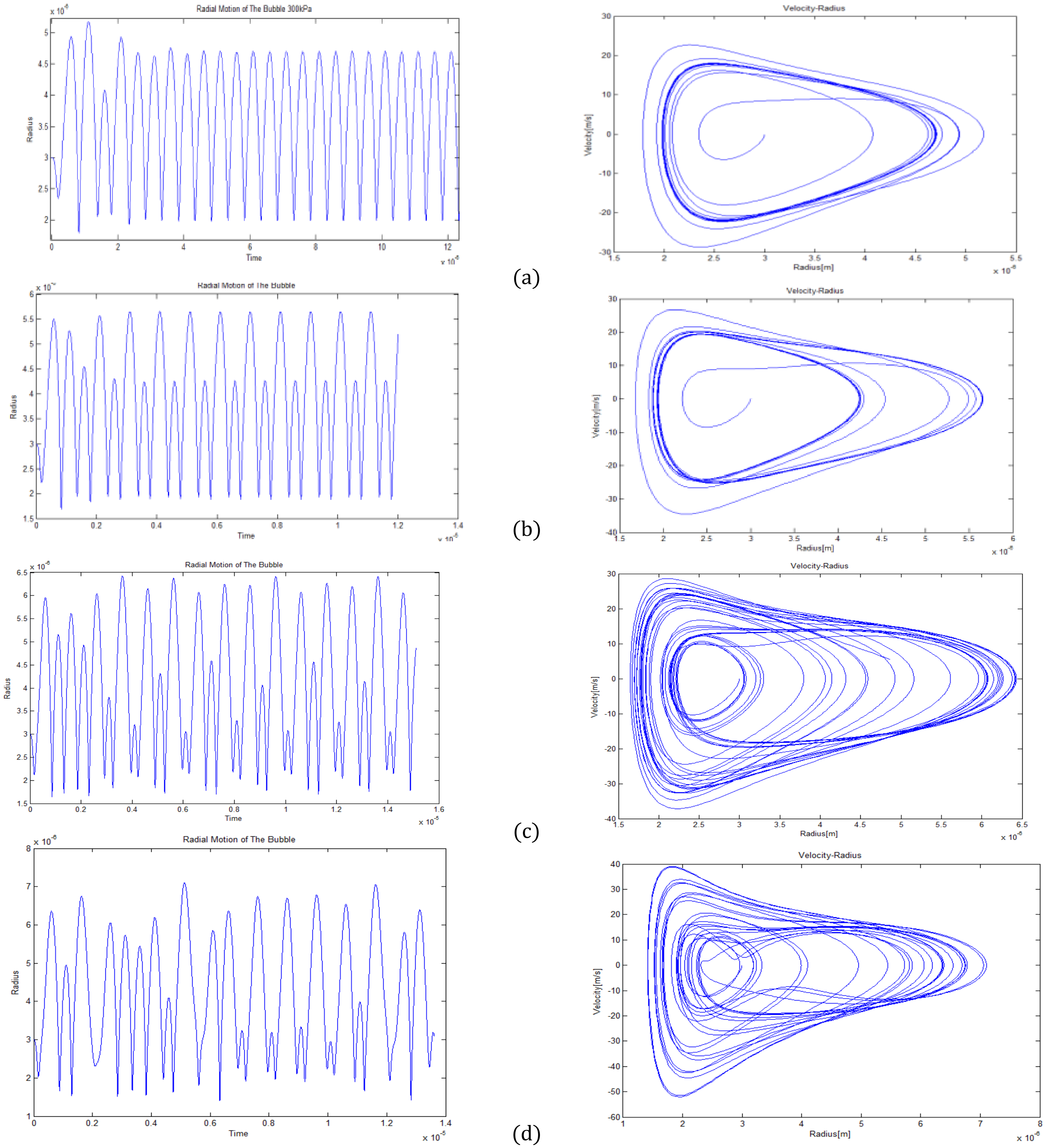

Fig. (3.3) Radius vs. time plots and Phase portraits of Sonazoid© UCA with f = 2 MHz, R_e=3 µm, For (a) Pac =300 kPa, (b) Pac =400 kPa, (c) Pac =450 kPa, and (d) Pac =500 kPa.

Bifurcation diagrams [6] provide a better perspective to identify exactly where the period doubles and when chaos occurs. The bifurcation diagram and Lyapunov exponents for the shells listed in Table (2.3) are calculated for four combinations of acoustic frequency and equilibrium radius, as presented in Hoff, over the acoustic pressure range of 10 kPa to 1MPa.

Figure (3.4) shows the bifurcation diagram along with the corresponding maximum Lyapunov exponent. At points where the period doubles, the Lyapunov exponent approaches zero, then decreases, indicating a bifurcation of the periodic orbit. The chaotic regions are indicated at a given acoustic pressure by spread on the bifurcation diagram, which corresponds to a positive Lyapunov exponent [6].

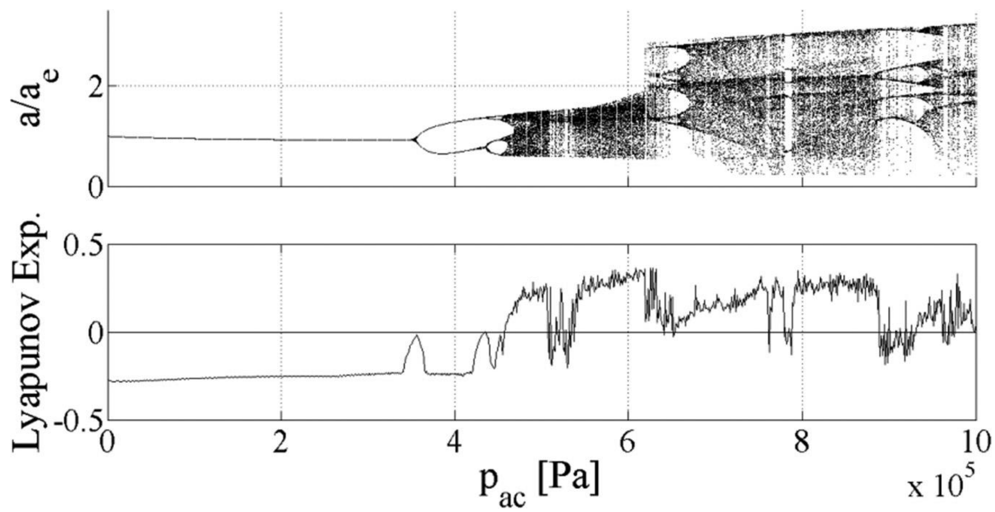

Fig.(3.4). Bifurcation diagram (upper figure) and maximum Lyapunov exponent (lower figure) for Sonazoid© UCA with f =2 MHz and R_e=3 μm.

2-3 Conclusion

We studied the chaotic motion of microbubble, and we noticed that by increasing pulse amplitude the bubble start in chaotic motion. And also we have examined the nonlinear response of spherical UCAs in typical clinical ranges of acoustic pressure and frequency.

Based on the results of this work, it is clear that the encapsulating material of the contrast agent significantly influences the dynamic response of the UCA to incident ultrasound.

Studying the chaotic motion will be important in the future research to develop a nonlinear control system to control the UCA response through modulation of the applied ultrasound.

References

1 M.S Plesset, A. Prosperetti, Bubble dynamics and cavitation, Ann. Rev. Fluid Mech 9, 145-185 (1977).

2 A. Doinikov and A. Bouakaz, “Review of shell models for contrast agent microbubbles,” IEEE Trans. Ultrason. Ferroelectr. Freq. Control 58(5), 981–993 (2011).

3 J.B. Keller and M. Miksis. Bubble oscillations of large amplitude. J Acoust Soc Am, 68(2):628–633, (1980).

4 T. Leighton, The Acoustic Bubble, Academic Press (1997)

5 Hoff, P. Sontum, and J. Hovem. Oscillations of polymeric microbubbles: Effect of the encapsulating shell. J Acoust Soc Am, 107(4):2272–2280, (2000).

6 M. Carroll, L. Calvisi and Leal K. Lauderbaugh, Dynamical analysis of the nonlinear response of ultrasound contrast agent microbubbles, Acoust Soc Am (2013)

7 P. Marmottant, S. van der Meer, M. Emmer, M. Versluis, N. de Jong, S. Hilgenfeldt, and D. Lohse, A model for large amplitude oscillations of coated bubbles accounting for buckling and rupture, J. Acoust. Soc. Am. 118, 3499–3505 (2005).

8 Katiyar et al, Modeling subharmonic response from contrast microbubbles as a function of ambient static pressure J. Acoust. Soc. Am. 129, 2325, 2335 (2011)

9 Jonathan Loughran et al, Modeling non-spherical oscillations and stability of acoustically driven shelled microbubbles, J. Acoust. Soc. Am. 131, 4349-4357 (2012)

10 Y. Liu et al, Numerical study on the shape oscillation of an encapsulated microbubble in ultrasound field, Phys. Fluids 23, 041904 (2011).

11 J.S. Allen and M.M. Rashid. Dynamics of a hyperelastic gas-filled spherical shell in a viscous fluid. J Appl Mech, 71:195–200, (2004).

12 B.A.J. Angelsen and R. Hansen. Surf imaging - a new method for ultrasound contrast agent imaging. In Proc IEEE Ultrasonics Symposium, pages 531–541, (2007).

13 H. Becher and P.N. Burns. Handbook of contrast echocardiography: LV function and myocardial perfusion. Springer-Verlag, Berlin, (2000).

14 M.A. Borden and M.L. Longo. Dissolution behavior of lipid monolayer-coated, air-filled microbubbles: Effect of lipid hydrophobic chain length. Langmuir, 18:9225–9233, (2002).

15 A. Bouakaz and N. de Jong. WFUMB safety symposium on echo-contrast agents: nature and types of ultrasound contrast agents. Ultrasound Med Biol, 33(2):187–196, (2007).

16 A. Bouakaz, S. Frigstad, F.J. Ten Cate, and N. de Jong. Super harmonic imaging: a new imaging technique for improved contrast detection. Ultrasound Med Biol, 28:59–68, (2002).

17 A. Bouakaz, M. Versluis, and N. de Jong. High-speed optical observations of contrast agent destruction. Ultrasound Med Biol, 31(3):391–399, (2005).

18 J. B. Keller and M. Miksis, ‘‘Bubble oscillations of large amplitude,’’ J.Acoust. Soc. Am.(1980)

19 D. Chatterjee and K. Sarkar. A newtonian rheological model for the interface of microbubble contrast agents. Ultrasound Med Biol, 29(12):1749–1757, (2003).

20 D. Chatterjee, K. Sarkar, P. Jain, and N.E. Schreppler. On the suitability of broadband attenuation measurement for characterizing contrast microbubbles. Ultrasound Med Biol, 31(6):781–6, (2005).

21 Q. Chen, J. Zagzebski, T. Wilson, and T. Stiles. Pressure-dependent attenuation in ultrasound contrast agents. Ultrasound Med Biol, 28(8):1041–51, 2002.

22 C.C. Church. The effects of an elastic solid surface layer on the radial pulsations of gas bubbles. J Acoust Soc Am, 97(3):1510–1521, (1995).

23 N. de Jong and L. Hoff. Ultrasound scattering properties of albunex microspheres. Ultrasonics, 31 (3):175–181, (1993).

24 N. de Jong, L. Hoff, T. Skotland, and N. Bom. Absorption and scatter of encapsulated gas filled microbubbles: theoretical considerations and some measurements. Ultrasonics, (1992).

25 N. de Jong, R. Cornet, and C.T. Lanc´ee. Higher harmonics of vibrating gas-filled microspheres. part one: simulations. Ultrasonics, 32(6):447–453, (1994).

26 N. de Jong, A. Bouakaz, and F.J. ten Cate. Contrast harmonic imaging. Ultrasonics, 40(1):567–573, (2002).

27 N. de Jong, M. Emmer, C.T. Chin, A. Bouakaz, F. Mastik, D. Lohse, and M. Versluis. “compression-only” behavior of phospholipid-coated contrast bubbles. Ultrasound Med Biol, 33(4):653–656,(2007).

28 Frinking PJ, Brochot J, Arditi M. ‚Subharmonic scattering of phospholipid-shell microbubbles at low acoustic pressure amplitudes. IEEE, (2010).

29 Fox, F. E. and Herzfield, K. F. Gas bubbles with organic skin as cavitation nuclei. J. Acoust. Soc. Am. (1954).

30 de Jong, N., Hoff, L., Skotland, T., and Bom, N. Absorption and scatter of encapsulated gas filled microspheres: theoretical considerations and some measurements. Ultrasonics (1992).

Appendix

MATLAB code

A-1 Resonance frequency for Rayleigh-Plesset equation, RPNNP, church Model and Newtonian shell

```
%% Resonance frequency
R0=[2:1e-3:10];
p0=101300; %reference pressure Pa
R0=R0*1e-6; %define vector of R0s
d=15e-9; %shell thickness
R01=R0; %inner radius
R02=R0+d; %outer radius
sigma=7;
sigma1=4;% Pa
sigma2= 0.5;% Pa
rho=1000; %fluid density kg/m3
rhoS= 1100; %shell density kg/m3
gamma=1.4; %polytropic exponent
Gs=88.8e6;% Pa
Vs=R02.^3-R01.^3;
alpha=(1+((rho-rhoS)/rhoS)*(R01./R02));
Z=(2*sigma1./R01+2*sigma2./R02).*(R02.^3./Vs)./(4*Gs);
w0rp=R0.^(-1)*sqrt(3*gamma*p0/rho); % rp resfreq.
w0rp=w0rp./1e6;
w0rpnnp=R0.^(-1).*sqrt((3*gamma*(p0+2*sigma./R0)-2*sigma./R0)/rho); %rpnnp
w0rpnnp=w0rpnnp./1e6;
%church:
w0sh2=(rhoS*R01.^2.*alpha).^(-1).*(3*gamma*p0-2*sigma1./R01-...
2*sigma2.*R01.^3./(R02.^4)+4*Vs*Gs./(R02.^3).*(1+Z.*(1+3*R01.^3./R02.^3)));
w0sh=sqrt(w0sh2);
w0sh=w0sh./1e6;
%newtonian shell
w0n2=(rhoS*alpha.*R01.^2).^(-1).*(3*(p0 + 2*sigma1./R01 ...
+2*sigma1./R02)*gamma-2*sigma1./R01-2*sigma2.*R01.^3./(R02.^4));
w0n=sqrt(w0n2);
w0n=w0n./1e6;
lstr1=['NF Shell ', num2str(d*1e9),'nm'];
lstr2=['VE Shell ', num2str(d*1e9),'nm'];
plot(R0, w0rp, 'r'),xlabel('Initial bubble radius, m'),ylabel('Resonant frequency, MHz'),title('Resonant frequency')
figure
plot( R0, w0rpnnp, 'g'),xlabel('Initial bubble radius, m'),ylabel('Resonant frequency, MHz'),title('Resonant frequency')
figure
```

```
plot( R0, w0sh, 'k',R0, w0rp, 'r'),xlabel('Initial bubble radius, m'),ylabel('Resonant frequency, MHz'),title('Resonant frequency')
figure
plot(R0, w0rp, 'r', R0, w0rpnnp, 'g',R0, w0n,'b', R0, w0sh, 'k')
h =legend('Rayleigh-Plesset equation ','RPNNP', lstr1, lstr2);
set(h,'Interpreter','none')
xlabel('Initial bubble radius, m')
ylabel('Resonant frequency, MHz')
title('Resonant frequency')
```

A-2 to create Ultrasound pulse in Hoff model

```
function [t,p]= BS_MakePulse(A,Nc,f0,fs,envelope)
% function [t,p]= BS_MakePulse(A,Nc,f0,fs,envelope)
%
%         A : Amplitude
%        Nc : No. of cycles
%        f0 : Centre frequency [Hz]
%        fs : Sample frequency [Hz]
%  envelope : Name of pulse envelope, windowing funtion
%
%   Construct ultrasound pulse
%-- Time ---
T = Nc/f0;                % Pulse length
dt= 1/fs;                 % Sample interval
tp= (0:dt:T )';           % Time vector, containing oscillations
t = (0:dt:4*T )';         % Time vector, total
%--- Pulse ---
W  = BS_Window( envelope{1}, length(tp), envelope{2});
po = sin(2*pi*f0*tp) ;     % Carrier wave
    po = A*po.*W;              % Pulse with envelope
%--- Place pulse ---
p= zeros( size(t) );
n= [1:length(po) ]; % Index to put oscillations into
p(n)= po;
return
```

A-3 Simulate Rayleigh-Plesset equation for gas encapsulated in a shell.

```
function dxv= BS_Rayleigh( T, xv, flag, Q, parameter )
% function dxv= BS_Rayleigh( T, xv, flag, Q, parameter )
%
% Simulate Rayleigh-Plesset equation for gas encapsulated
% in a shell
% Written for Matlab's ODE solvers
% Normalized radial displacement, pressure and time
% T     : Normalized time T = t*w0, w0= sqrt(p0/(rho*a0^2))
% x     : Radial displacement  a(t)= a0(1+x)
% flag  : Parameters for ODE solver, not used
% Q     : Normalized acoustic pressure: P= p(t)/p0
% parameter : Normalized visco-elastic parameters
qi= interp1( Q.t, Q.p, T, '*cubic' );   % Driving pressure
x = xv(1,:);  % Strain
dx= xv(2,:);  % Velocity
%--- Physical parameters ---
gs   = parameter.gs;
ns   = parameter.ns;
nL   = parameter.nL;
kappa= parameter.k;

%--- Pressure at bubble surface ---
[qL,q1,q2]= BS_SurfacePressure(x,dx,gs,ns,nL,kappa);
```

```
%--- ODE ---
q3 =  1+x;
ddx= -1./q3.*(3/2*dx.^2 +1+qi-qL );
%--- ODE as vector equation ---
dxv= [dx; ddx];
return
```

A-4 Simulate Rayleigh-Plesset equation with damping.

```
function dxv= BS_ModifiedRayleigh( T, xv, flag, pi, parameter )
% function dxv= BS_ModifiedRayleigh( T, xv, flag, pi, parameter )
% Simulate modified Rayleigh-Plesset equation for gas encapsulated in a shell
% Equation modified by adding radiation damping term, dp/dt
% Written for Matlab's ODE solvers
% Normalized radial displacement, pressure and time
%
% T     : Normalized time T = t*w0, w0= sqrt(p0/(rho*a0^2))
% x     : Radial displacement  a(t)= a0(1+x)
% flag  : Parameters for ODE solver, not used
% pi    : Normalized acoustic pressure: P= p(t)/p0
% parameter : Normalized bubble and liquid parameters
qi= interp1( pi.t, pi.p, T, '*cubic' );   % Driving pressure
x = xv(1,:);  % Strain
dx= xv(2,:);  % Velocity
 %--- Physical parameters ---
gs   = parameter.gs;
ns   = parameter.ns;
nL   = parameter.nL;
cn   = parameter.c;
kappa= parameter.k;
%--- Pressure at bubble surface ---
[qL,q1,q2]= BS_SurfacePressure(x,dx,gs,ns,nL,kappa);
%--- ODE ---
q3 = (1+x) -1/cn.*(1+x).*q2;
ddx=-1./q3.*(3/2*dx.^2 -1/cn*(1+x).*q1.*dx +1+qi-qL );
%--- ODE as vector equation ---
dxv= [dx; ddx];
return
```

A-5 Solution of Rayleigh-Plesset equation .

```
[T,R]=ode45('BS_Rayleigh', [0 3e-6], [1e-6 70]);
plot(T,R(:,1),'-o')
```

A-6 Simulation of the Pressure at the bubble surface

```
function [qL,q1,q2]= BS_SurfacePressure(x,dx,gs,ns,nL,kappa);
% function [qL,q1,q2]= BS_SurfacePressure(x,dx,gs,ns,nL,kappa);
% Pressure at the bubble surface
%   x : Radial strain
%  dx = dx/dt
%  gs : Normalized shell shear modulus
%  ns : Normalized shell shear viscosity
%  nL : Normalized liquid viscosity
%  kappa: Polytropic exponent
%  qL : Pressure at bubble surface
%  q1 = dqL/dx
%  q2 = dqL/ddx
%  Calcualate pressure at bubble surface
%  Boundary condition for ODE giving bubble motion
%--- Gas pressure ---
qg = (1+x).^(-3*kappa);
dqg= -3*kappa*(1+x).^(-3*kappa-1);
```

```
%--- Shell pressure ---
%--- Exponential shell model ---
x0= 1/8; eg= exp(-x/x0);  % Stiffness
x1= 1/4; en= exp(-x/x1);  % Viscosity
qs  = -12*( gs*x0*(1-eg) + ns   *en.*dx);
dqs1= -12*( gs*eg        - ns/x1*en.*dx);
dqs2= -12*ns*en;
%--- Pressure at bubble wall ---
qL =-4*nL*dx./(1+x)    +  qs + qg;
q1 = 4*nL*dx./(1+x).^2 +dqs1 +dqg;
q2 =-4*nL* 1./(1+x)    +dqs2;
return
```